Thermal Conductivity of HFC-245fa from (243 to 413) K

Yugang Wang, Jiangtao Wu,* Zhengxin Xue, and Zhigang Liu

State Key Laboratory of Multiphase Flow in Power Engineering, Xi'an Jiaotong University, Xi'an Shaanxi 710049, People's Republic of China

The thermal conductivity of 1,1,1,3,3-pentafluoropropane (HFC-245fa) was measured in both the saturated liquid and the vapor phase by the transient double hot-wire method. Measurements of the thermal conductivity of the saturated liquid HFC-245fa were reported over the temperature range from (243 to 413) K while in vapor phase were from (293 to 413) K along 13 quasi-isotherms and at pressures up to saturation. The total uncertainly of the experiment was less than ± 2.0 %. The results of liquid phase were correlated as a function of temperature as well as the gas-phase results were correlated as a function of temperature and pressure. The standard and maximum deviations of the liquid experimental results from the correlation were less than 0.21 % and −0.56 %, respectively. The maximum deviation and the absolute mean deviation of the gaseous measured data from its equation were 0.87 % and 0.38 %, respectively.

Introduction

Some replacements for chlorofluorocarbon (CFC) were developed recently using HCFCs (hydrochlorofluorocarbons) and HFCs (hydrofluorocarbons). Thus, it's not difficult to understand the commercialization of the HFCs. The thermophysical properties and environmental characteristics of HFC-245fa make it suitable for a number of applications such as centrifugal chillers for comfort cooling, Rankine Cycle for energy recovery and power generation, and sensible heat transfer in low-temperature refrigeration. It also has zero ozone depletion potential and a low global warming potential. So, this refrigerant is currently considered to be a promising replacement for chlorine-containing compounds such as 1,1-dichloro-1-fluoroethane (R-141b) and 1,2-dichloro-1,1,2,2-tetrafluoroethane (R-114).

For serious application, the availability of its physical properties is a necessity. Several publications have already dealt with the viscosity, static dielectric constant, and compressed and saturated liquid densities. But there appear to be few data of the liquid-phase and gaseous thermal conductivity of HFC-245fa in the literature.[1−3] In this work, the thermal conductivities of the saturated liquid HFC-245fa over the temperature range from (243 to 413) K and gaseous HFC-245fa from (293 to 413) K at pressures up to 2500 kPa are reported.

Experimental Section

The transient hot-wire technique is widely recognized as the most accurate method for the measurement of the thermal conductivity of fluids. The fundamental working equation of the transient hot-wire method takes the form:[4]

$$\lambda(T_r, P) = (q/4\pi)(\mathrm{d}\Delta T_{id}/\mathrm{d}\ln t) \tag{1}$$

where q is the power input per unit length of wire, $\lambda(T_r, P)$ is the thermal conductivity of the fluid at a reference temperature T_r and at the working pressure P, $\mathrm{d}\Delta T_{id}/\mathrm{d}\ln t$ is the slope of a line fit to the temperature rise in an ideal condition ΔT_{id} versus $\ln t$ data, where t represents the elapsed time. The ideal temperature rise is obtained by considering a number of corrections δT_i to the experimental temperature rise ΔT_{exp} according to

$$\Delta T_{id} = \Delta T_{exp} + \sum_i \delta T_i \tag{2}$$

The corrections $\sum \delta T_i$ have been described in refs 5, 6, and 7. In this work, the corrections concern mostly about the properties of the wire. The reference temperature T_r associated with a given thermal conductivity data point is given by

$$T_r = T_0 + (\Delta T_1 + \Delta T_2)/2 \tag{3}$$

where T_0 is the initial temperature; ΔT_1 and ΔT_2 are the temperature rise at the start time and the end time of the linear region selected for the regression.

The schematic diagram of the transient hot-wire apparatus was shown in Figure 1. Two platinum wires which were of 15 μm in nominal diameter and (150 and 50) mm in length were used. A spring was used to ensure a constant tension on the platinum wire. The calibration of the resistance-temperature relation of the platinum wire was carried out in situ in the temperature range from (243 to 413) K. The maximum deviation and the average absolute deviation of the measured values from the correlated equation of the resistance temperature relation were 0.1 % and 0.05 %, respectively. The apparatus and connections were all made of stainless steel (1Cr18Ni9Ti), and the total volume was about 180 mL calibrated with water.

The measurement circuit is shown in Figure 2, which consists of several components:[8] a Wheatstone bridge, an Advantech PCL-818HG high-precision DAQ card, a high-speed analogue switch (model MAX303), an Agilent E3617A dc power supply, and an industrial computer.

The transient hot-wire apparatus was immersed completely in a thermostatic bath. The methyl silicon oil was selected as the bath fluid for the temperature range from (243 to 413) K. The temperature stability of the thermostatic bath was better than ± 4 mK·h^{-1}. The temperature was measured with an ASL's

* Corresponding author. E-mail: jtwu@mail.xjtu.edu.cn. Fax: +86-29-82668789.

10.1021/je060116w CCC: $33.50
Published on Web 06/27/2006

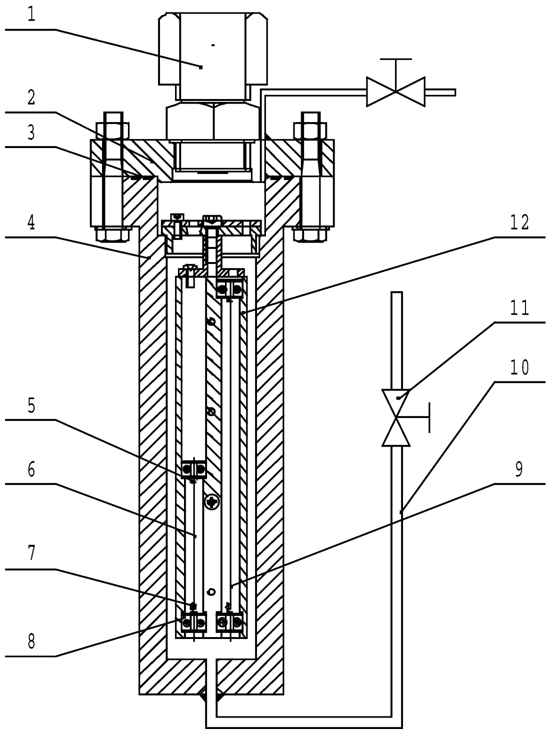

Figure 1. Hot-wire assembly: 1, conax seal; 2, flange; 3, Teflon seal; 4, pressure vessel; 5, gold terminal; 6, short wire; 7, weight/spring; 8, fastening component; 9, long wire; 10, pipeline; 11, valve; 12, cell.

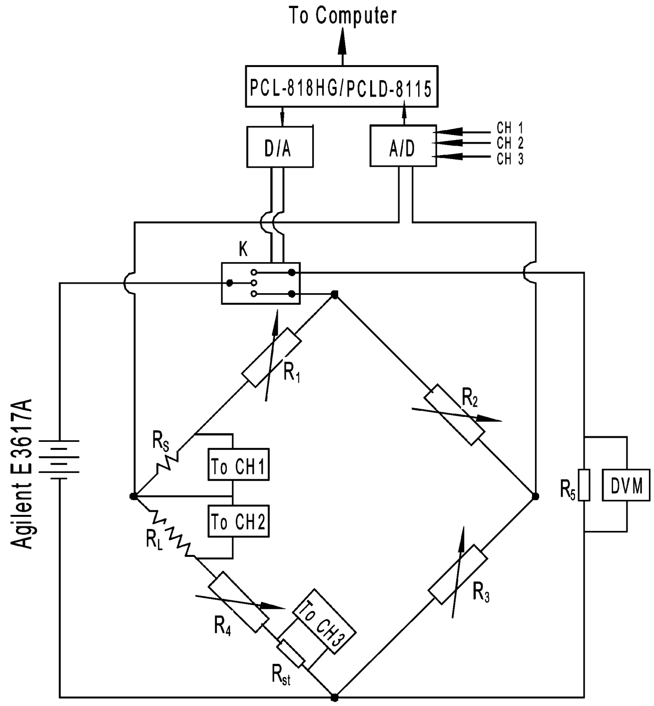

Figure 2. Circuit diagram for the transient hot-wire apparatus.

F18 ac thermometry bridge and a 25.5 Ω standard platinum resistance thermometer. The total uncertainty of temperature for thermal conductivity was less than ± 10 mK (ITS-90) with a coverage factor of $k = 2$. For pressure measurement, a high-precision quartz pressure sensor (Paroscientific Inc., model 42K-101) and a differential pressure transducer (Rosemount, model 3051) were used. The range of pressure measurement was from (0 to 13.8) MPa. The total uncertainty of pressure for thermal conductivity was less than ± 1.5 kPa. The details about the thermostatic bath, the temperature measurement, and the pressure measurement have been given in previous papers.[9,10]

The overall standard uncertainty of the present thermal conductivity measurements was estimated to be better than ± 2.0 %; the details were given in ref 8.

Results and Analysis

Before the apparatus was used to measure the thermal conductivity of HFC-245fa, the performance of the apparatus was checked by toluene and nitrogen. In addition, the thermal conductivity of dimethyl ether was also measured by this apparatus.[8]

The sample of HFC-245fa was provided by Zhejiang Fluoro-Chemical Technology Research Institute. The mass fraction purity of HFC-245fa was better than 99.9 %, as indicated by analysis with gas chromatograph (Agilent Technologies, model 6890N). A flame ionization detector (FID) and a capillary column (GS-GASPRO, model Agilent 113-4362) were used for the analysis with the carrier gas hydrogen at 4.0 mL/min, and the oven temperature and the detector temperature were 423 K and 473 K, respectively.

The thermal conductivity of liquid HFC-245fa was measured at temperatures ranging from (243 to 413) K near the saturated

Table 1. Experimental Data of the Thermal Conductivity of Saturated Liquid HFC-245fa

T_r	λ_{exp}	λ_{FEM}	q	T_r	λ_{exp}	λ_{FEM}	q	T_r	λ_{exp}	λ_{FEM}	q
K	$mW \cdot m^{-1} \cdot K^{-1}$	$mW \cdot m^{-1} \cdot K^{-1}$	$mW \cdot m^{-1}$	K	$mW \cdot m^{-1} \cdot K^{-1}$	$mW \cdot m^{-1} \cdot K^{-1}$	$mW \cdot m^{-1}$	K	$mW \cdot m^{-1} \cdot K^{-1}$	$mW \cdot m^{-1} \cdot K^{-1}$	$mW \cdot m^{-1}$
244.40	104.4	106.2	242.74	305.08	85.42	86.15	327.10	355.37	70.58	71.58	296.09
244.64	104.3	106.2	289.14	314.17	82.60	83.33	162.77	364.67	66.48	67.00	200.37
244.90	104.1	106.2	340.18	314.45	82.76	83.36	206.22	365.04	66.36	67.00	247.47
254.41	101.4	103.0	244.78	314.53	82.59	83.36	221.96	365.43	66.04	67.00	299.79
254.67	101.4	102.9	291.60	314.76	82.69	83.34	255.35	374.69	63.71	63.65	196.52
254.94	101.3	103.0	342.94	314.80	82.62	83.36	263.56	375.06	63.10	63.65	242.67
264.37	98.35	99.50	238.63	315.13	82.52	83.36	311.11	375.44	62.62	63.60	293.55
264.64	98.20	99.50	290.43	315.17	82.34	83.35	320.20	384.70	61.17	61.04	192.42
264.91	98.10	99.50	340.60	324.46	79.50	80.53	201.89	385.14	60.60	61.04	237.41
274.38	95.19	95.96	237.82	324.78	79.45	80.53	250.23	385.48	59.85	61.04	287.89
274.66	95.25	95.96	288.56	325.15	79.53	80.52	304.08	394.71	58.33	58.20	188.79
274.94	94.97	95.96	338.43	334.52	76.49	77.50	197.31	395.10	58.13	58.20	233.13
284.51	92.19	92.78	232.78	334.84	76.50	77.50	244.69	395.52	57.83	58.20	282.62
284.80	92.11	92.78	282.18	335.21	76.50	77.50	297.80	404.77	55.98	55.84	185.60
285.08	91.78	92.76	330.66	344.59	73.65	74.55	202.18	405.12	55.95	56.24	228.76
294.42	88.94	89.54	232.20	344.93	73.51	74.55	249.16	405.54	55.64	56.14	276.67
294.67	88.95	89.54	275.46	345.31	73.56	74.55	301.98	414.79	53.31	53.50	188.79
294.99	88.62	89.54	328.51	354.66	70.59	71.59	200.32	415.16	53.16	53.30	224.36
304.46	85.98	86.15	227.58	355.00	70.59	71.59	246.01	415.54	52.90	53.20	271.06
304.72	85.64	86.15	270.13								

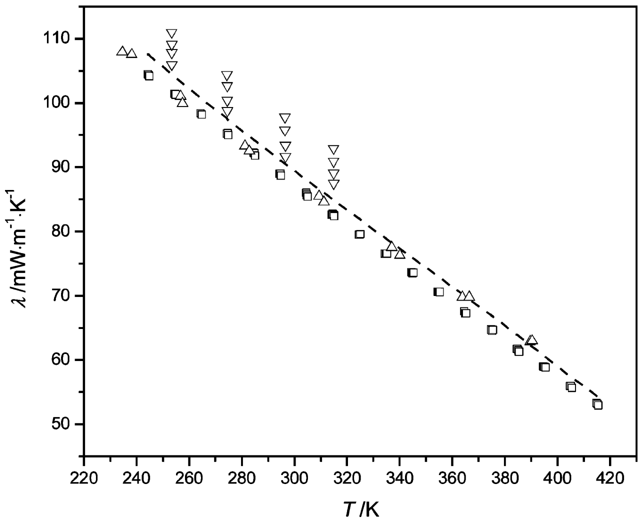

Figure 3. Thermal conductivity of saturated liquid HFC-245fa vs temerature: □, this work; - - -, REFPROP 7.0;[11] △, Geller et al.;[1] ▽, Yata et al.[2]

line. The state can be determined through monitoring the pressure in the cell by the pressure measurement system. The results are listed in Table 1 and illustrated in Figure 3 where the comparisons are made between these experimental data and those of Geller et al.[1] and Yata et al.[2] The λ_{exp} values represented here are the averages of several runs at the same heat power q, and its repeatability at the same temperature and pressure was better than ± 0.5 %.

In this work, the experimental values of the thermal conductivity of liquid HFC-245fa were correlated as the function of temperature using a least-squares method to the following equation:

$$\lambda/\mathrm{mW\cdot m^{-1}\cdot K^{-1}} = 1.887386 \times 10^{2} - 3.693486 \times 10^{-1}(T/\mathrm{K}) + 1.02339210^{-4}(T/\mathrm{K})^{2} \quad (4)$$

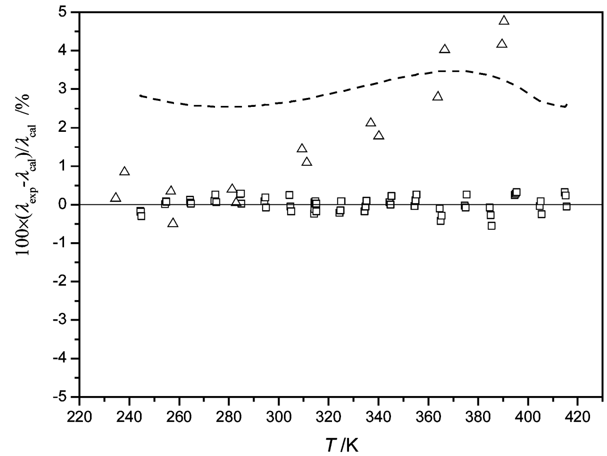

Figure 4. Relative deviations of the experimental thermal conductivity data from eq 4: □, this work; - - -, REFPROP 7.0;[11] △, Geller et al.[1]

The deviations of the experimental data from eq 4 are shown in Figure 4. The maximum deviation and the mean deviation of this experimental data from eq 4 are −0.56 % and 0.21 %, respectively. Below 300 K, the deviations of Geller et al.[1] from eq 4 were within 1.0 %; however, above 300 K, it increases rapidly and reaches about 4.8 % at 390 K. The deviations between the NIST REFPROP 7.0 and eq 4 were about 3.0 % from (240 to 410) K. The equation of REFPROP 7.0 was fitted with the experimental data from refs 1 to 3. The average absolute deviations of the REFPROP 7.0 from the experimental data were 1.30 %,[2] 2.63 %,[3] and 7.80 %,[1] and the overall was 6 %.[11] It was indicated that these data had the agreement under the measurement uncertainties.

In addition, the numerical FEM method is also used to solve the energy conservation partial-differential set of equations that describes the transient hot-wire theory. The details could be referred to refs 12 and 13. During the calculation, a 1134 elements, 2-D rectangle variable size mesh was assumed. The

Table 2. Experimental Data of the Thermal Conductivity of Gaseous HFC-245fa

T_r / K	P / kPa	λ_{exp} / $\mathrm{mW\cdot m^{-1}\cdot K^{-1}}$	q / $\mathrm{mW\cdot m^{-1}}$	T_r / K	P / kPa	λ_{exp} / $\mathrm{mW\cdot m^{-1}\cdot K^{-1}}$	q / $\mathrm{mW\cdot m^{-1}}$	T_r / K	P / kPa	λ_{exp} / $\mathrm{mW\cdot m^{-1}\cdot K^{-1}}$	q / $\mathrm{mW\cdot m^{-1}}$
296.14	121.3	12.56	43.51	375.13	604.2	19.56	48.29	405.12	604.3	22.48	54.08
297.06	121.3	12.57	43.51	375.71	604.2	19.59	61.88	405.62	604.3	22.49	67.38
297.76	121.3	12.67	57.29	376.31	604.2	19.63	76.43	406.18	604.3	22.53	82.64
305.45	123.2	13.42	34.49	374.99	997.0	19.66	48.64	405.00	998.4	22.48	53.78
305.99	123.2	13.45	42.44	375.48	997.0	19.69	61.51	405.48	998.4	22.53	67.15
306.63	123.2	13.52	51.48	376.05	997.0	19.76	76.73	406.02	998.4	22.70	82.70
315.24	203.4	14.25	33.85	374.84	1243.0	19.82	48.48	404.85	1500.7	22.77	53.84
315.99	203.4	14.28	45.82	375.31	1243.0	19.95	61.80	405.30	1500.7	22.85	67.50
316.55	203.4	14.35	54.88	375.83	1243.0	20.01	76.62	405.78	1500.7	23.02	82.44
325.29	203.3	15.20	36.55	385.20	598.1	20.52	51.60	404.75	1999.2	23.62	58.17
326.02	203.3	15.24	49.05	385.76	598.1	20.59	65.28	405.14	1999.2	23.64	88.45
326.56	203.3	15.27	58.00	386.35	598.1	20.60	80.54	405.55	1999.2	23.69	72.26
335.28	291.6	16.07	39.73	385.04	998.9	20.61	51.71	404.55	2269.8	24.83	58.00
335.96	291.6	16.10	52.19	385.55	998.9	20.67	65.20	404.89	2269.8	24.75	72.36
336.77	291.6	16.11	66.87	386.13	998.9	20.72	80.65	405.29	2269.8	24.84	88.33
345.15	303.0	17.04	39.04	384.79	1489.1	21.10	51.67	415.15	604.1	23.37	57.03
345.77	303.0	17.10	51.28	385.21	1489.1	21.01	65.25	415.64	604.1	23.46	71.06
346.50	303.0	17.14	65.33	385.68	1489.1	21.12	80.47	416.19	604.1	23.48	86.57
355.04	579.7	17.78	42.13	395.07	602.5	21.48	50.75	415.04	995.9	23.42	57.03
355.63	579.7	17.82	54.78	395.58	602.5	21.53	63.69	415.68	995.9	23.55	76.16
356.29	579.7	17.91	69.51	395.94	602.5	21.47	73.66	416.22	995.9	23.60	92.56
354.97	738.2	17.82	42.13	395.09	1004.6	21.49	54.91	415.04	1502.2	23.74	61.64
356.17	738.2	17.90	69.20	395.60	1004.6	21.61	68.84	415.64	1502.2	23.78	81.08
355.53	738.2	17.86	54.88	396.04	1004.6	21.68	81.23	416.18	1502.2	23.99	98.41
365.05	617.9	18.65	44.65	394.90	1498.3	22.08	54.92	414.88	1998.0	24.56	61.63
365.61	617.9	18.73	57.61	395.36	1498.3	22.16	68.76	415.45	1998.0	24.60	81.09
366.24	617.9	18.78	72.15	395.75	1498.3	22.18	81.13	415.92	1998.0	24.67	98.06
364.88	954.5	18.76	44.57	394.74	1765.3	22.46	54.86	414.76	2496.6	26.64	66.31
365.40	954.5	18.75	57.72	395.16	1765.3	22.51	68.89	415.25	2496.6	26.94	86.66
365.96	954.5	18.90	71.90	395.52	1765.3	22.58	81.49	415.66	2496.6	26.96	104.17

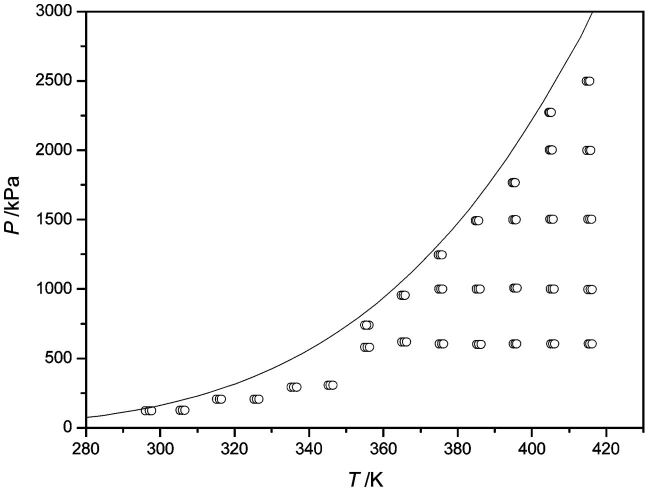

Figure 5. Temperature and pressure ranges for the gaseous experimental points: ○, measured state point; −, saturated vapor pressure.

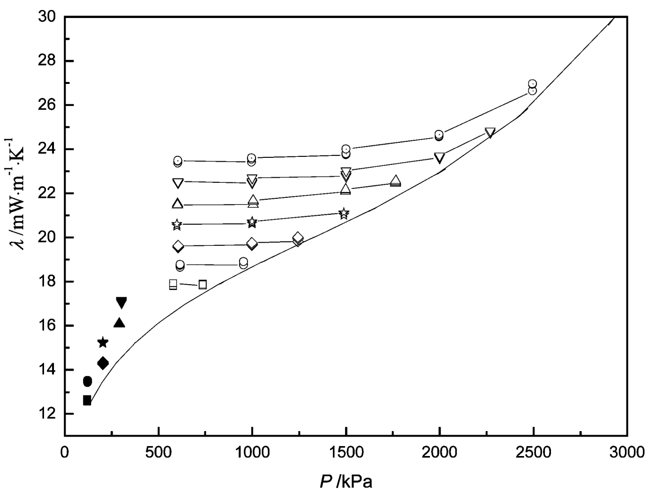

Figure 6. Thermal conductivity of gaseous HFC-245fa vs pressure near different isotherms: ■, 293.15 K; ●, 303.15 K; ♦, 313.15 K; ★, 323.15 K; ▲, 333.15 K; ▼, 343.15 K; □, 353.15 K; ○, 363.15 K; ◇, 373.15 K; ☆, 383.15 K; △, 393.15 K; ▽, 403.15 K; ◎, 413.15 K.

Table 3. Coefficients Used in Equations 5, 6, and 7

coefficient	value	coefficient	value
a_0	-1.43644×10^{1}	c_0	4.809115×10^{4}
a_1	9.06916×10^{-2}	c_1	-8.583926×10^{2}
b_2	2.48448×10^{-8}	c_2	6.373297×10^{0}
b_3	-1.20770×10^{-11}	c_3	-2.519650×10^{-2}
b_4	9.11801×10^{-14}	c_4	5.595359×10^{-5}
		c_5	-6.618411×10^{-8}
		c_6	3.258104×10^{-11}

differences of the thermal conductivity of liquid HFC-245fa calculated by FEM and traditional method are shown in Table 1. The maximum deviation is 2.0 %, and the average deviation is 0.97 %. It indicated that the results were in agreement if the uncertainty was 2.0 %.

The thermal conductivity of gaseous HFC-245fa was measured at temperatures ranging from (293 to 413) K and at pressures up to saturation. The maximum pressure was 2500 kPa. Totally 90 data points were obtained along 13 quasi-isotherms, and the distribution in temperature−pressure diagram is shown in Figure 5 where the saturated vapor pressures are from ref 14. The results are listed in Table 2 and illustrated in Figure 6. The λ_{exp} values represented here are the averages of several runs at the same heat power, whose repeatability at the same temperature and pressure was better than ± 0.5 %.

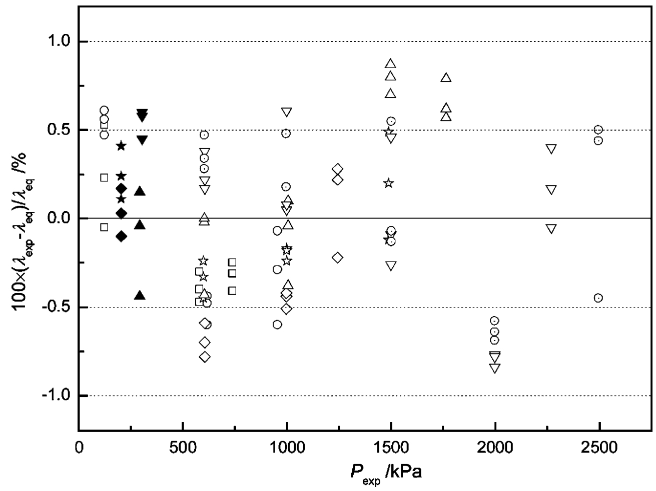

Figure 7. Relative deviations of the experimental thermal conductivity data from eq 5 (plotted vs pressure): ■, 293.15 K; ●, 303.15 K; ♦, 313.15 K; ★, 323.15 K; ▲, 333.15 K; ▼, 343.15 K; □, 353.15 K; ○, 363.15 K; ◇, 373.15 K; ☆, 383.15 K; △, 393.15 K; ▽, 403.15 K; ◎, 413.15 K.

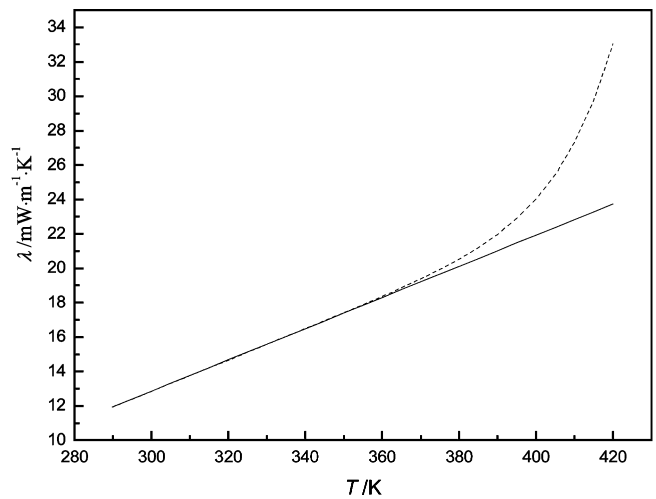

Figure 8. Thermal conductivity of the saturation vapor and the ideal gas of HFC-245fa: −, dilute gas; - - -, saturated vapor.

In this work, the experimental values of the thermal conductivity of gaseous HFC-245fa were correlated as the function of temperature and pressure using a least-squares method to the following equation:

$$\lambda/\mathrm{mW{\cdot}m^{-1}{\cdot}K^{-1}} = a_0 + a_1(T/\mathrm{K}) + \sum_{i=2}^{4} b_i(P/\mathrm{kPa})^i \qquad (5)$$

and the coefficients are listed in Table 3. The deviations between the experimental and calculated values are shown in Figure 7, where they are plotted as a function of pressure. The maximum deviation and the mean deviation of experimental data from eq 5 are 0.87 % and 0.38 %, respectively.

The comparisons between the experimental and calculated data from eq 5 are shown in Figure 9. The maximum deviation of this experimental data from eq 5 was within 1 %. It can be found that the Geller data were all lower while the NIST data were higher than this work and the values calculated from eq 5. Dohrn et al.[3] only provided four data that were all of 100 kPa, and they were bigger than the corresponding data provided by this work. However, all the maximum deviations were within 10 %.

In practical applications, the thermal conductivities for the saturation vapor as well as for the dilute gas ($\rho \rightarrow 0$ or $P \rightarrow 0$)

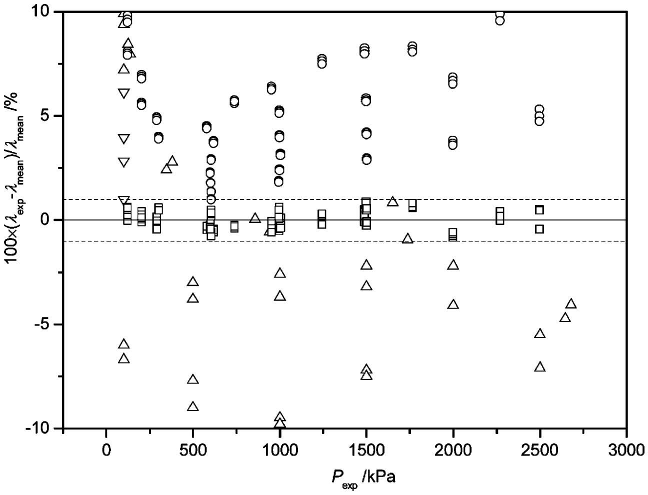

Figure 9. Relative deviations of the thermal conductivity data from eq 5: □, this work; ○, calculated with REFPROP 7.0;[11] △, Geller et al.;[1] ▽, Dohrn et al.[3]

are of special interest. Therefore, the thermal conductivity for saturated vapor and for dilute gas, indicated by λ_s and λ_0 respectively, are correlated by

$$\lambda_s/\text{mW}\cdot\text{m}^{-1}\cdot\text{K}^{-1} = \sum_{i=0}^{6} c_i(T/\text{K})^i \tag{6}$$

$$\lambda_0/\text{mW}\cdot\text{m}^{-1}\cdot\text{K}^{-1} = a_0 + a_1(T/\text{K}) \tag{7}$$

where the coefficients are also listed in Table 3. Considering that the upper-limit pressure is very close to the saturated pressure, which was measured with the high accuracy,[2] and the lower-limit pressure is about 150 kPa, the uncertainty of the extrapolated thermal conductivity of saturated vapor and dilute gas should be close to that of the measurements and could be regarded as ± 2.0 % in this work. The applicable temperature range of eq 6 and eq 7 is from (293 to 413) K. Finally, the thermal conductivity for saturated vapor and for dilute gas is plotted as a function of temperature in Figure 8.

Conclusions

Using a transient hot-wire apparatus, the thermal conductivity of HFC-245fa was measured in the temperature range from (243 to 413) K for saturated liquid and from (293 to 413) K along 13 quasi-isotherms and at pressures up to 2500 kPa for the gaseous phase, respectively. The uncertainty of the results is ± 2.0 %. The saturated liquid data were correlated as a function of temperature with the mean deviation 0.21 % and a maximum deviation −0.56 %. The gaseous measured data were correlated as a function of temperature and pressure with the mean deviation 0.38 % and a maximum deviation 0.87 %. For practical applications, the equations for saturated gas and dilute gas were also derived.

Acknowledgment

We are very thankful for Prof. Marc Assael's kind help and beneficial suggestions.

Literature Cited

(1) Geller, V.; Bivens, D. B.; Yokozeki, A. Transport properties and surface tension of hydrofluorocarbons HFC236fa and HFC 245fa. *Proceedings of the 20th International Congress of Refrigeration*, IIR/IIF, Sydney,1999.
(2) Yata, J.; Hori, M.; Niki, M.; Isono, Y.; Yanagitani, Y. Coexistence curve of HFC-134a and thermal conductivity of HFC-245fa. *Fluid Phase Equilib.* **2000**, *174*, 221−229.
(3) Dohrn, R.; Treckmann, R.; Heinemann, T. Vapor-phase thermal conductivity of 1,1,1,2,2-pentafluoropropane, 1,1,1,3,3-pentafluoropropane, 1,1,2,2,3-pentafluoropropane and carbon dioxide. *Fluid Phase Equilib.* **1999**, *159*, 1021−1028.
(4) Carslaw, H. S.; Jaeger, J. C. *Conduction of Heat in Solids*, 2nd ed.; Oxford University Press: London, 1959.
(5) Wakeham, W. A.; Nagashima, A.; Sengers, J. V. *Experimental Thermodynamics Vol. III*, *Measurement of the Transport Properties of Fluids*; Blackwell Scientific Publications: Oxford, 1991.
(6) Healy, J. J.; De Groot, J. J.; Kestin, J. The theory of the transient hot-wire method for measuring thermal conductivity. *Physica* **1976**, *82C*, 392−408.
(7) Wang, Y. G. Experimental research of thermal conductivity of liquid using transient two hot-wires method. Ph.D. Dissertation, Xi'an Jiaotong University, Xi'an, People's Republic of China, 2005.
(8) Wang, Y. G.; Wu, J. T.; Liu, Z. G. Thermal conductivity of gaseous dimethyl ether from (263 to 383) K. *J. Chem. Eng. Data* **2006**, *51*, 164−168.
(9) Wu, J. T. Development of the new thermophysical properties measurement system and research of thermophysical properties of dimethyl ether. Ph.D. Dissertation, Xi'an Jiaotong University, Xi'an, People's Republic of China, 2003.
(10) Wu, J. T.; Liu, Z. G.; Pan, J. Development of fluid thermophysical property measurement system with high accuracy. *J. Xi'an Jiaotong Univ.* **2004**, *38*, 937−942.
(11) Lemmon, E. W.; McLinden, M. O.; Huber, M. L. Reference fluid thermodynamic and transport properties. *NIST Standard Reference Database 23 (REFPROP), version 7.0*; National Institute of Standard and Technology: Boulder, CO, 2003.
(12) Assael, M. J.; Karagiannidis, L.; Malamataris, N.; Wakeham, W. A. The transient hot-wire technique: a numerical approach. *Int. J. Thermophys.* **1998**, *2* (19), 379−388.
(13) Assael, M. J.; Dix, M.; Gialou, K.; Vozar, L.; Wakeham, W. A. Application of the transient hot-wire technique to the measurement of the thermal conductivity of solids. *Int. J. Thermophys.* **2002**, *3* (23), 615−633.
(14) Pan, J.; Wu, J. T.; Liu, Z. G. Vapor Pressure of dimethoxymethane and 1,1,1,3,3-pentaflouropropane. *J. Chem. Eng. Data* **2006**, *51*, 186−189.

Received for review March 11, 2006. Accepted May 21, 2006. This work has been supported by the National Science Foundation of China (Grant 50306021).

JE060116W